

Supplementary Information

Deciphering the Role of Acid-Treated Clay Towards Selective Catalysis of Glucose to HMF

Preeti Kang^a, Matej Gabrijelčič^b, Andraž Krajnc^b, Blaž Likozar^{*b}, and Rakesh K Sharma^{*a}

^aSustainable Materials and Catalysis Research Laboratory (SMCRL), Department of Chemistry, Indian Institute of Technology Jodhpur, 342037-Jodhpur, India

^bNational Institute of Chemistry, Ljubljana, 1001, Slovenia.

*Corresponding author

E-mail address: rks@iitj.ac.in, blaz.likozar@ki.si

Number of pages: 24

Number of figures: 19

Content	Page no.
Materials and general characterization	S3
Catalysts preparation, catalytic conversion, and product analysis	S4
Catalyst recyclability	S5
Figure S1. XRD patterns of the untreated clay (CL) and after activation with acetic acid (AA-CL), formic acid (FA-CL), and malonic acid (MA-CL).	S6
Figure S2. N ₂ adsorption-desorption isotherms of CL, AA-CL, FA-CL, and MA-CL.	S7
Figure S3. Zeta potential measurements of CL, AA-CL, FA-CL, and MA-CL.	S8
Figure S4. FTIR spectra of CL, AA-CL, FA-CL, MA-CL.	S9
Figure S5. TGA profiles of CL, AA-CL, FA-CL, and MA-CL.	S10
Figure S6. Pyridine-FTIR spectra of CL, AA-CL, FA-CL, MA-CL.	S11
Figure S7. Effect of solvent amount on glucose conversion and HMF yield over FA-CL catalyst.	S12
Figure S8. Effect of catalyst dosage on glucose conversion and HMF yield over FA-CL catalyst.	S13
Figure S9. (a) HPLC chromatogram of crude product after 6 h of catalytic conversion of glucose over FA-CL catalyst. (b) HPLC chromatogram of purified HMF.	S14
Figure S10. ¹ H-NMR spectrum of purified HMF.	S15
Figure S11. HRMS data of (a) crude product and (b) purified HMF after 6 h of catalytic conversion of glucose over FA-CL catalyst.	S16
Figure S12. TGA of FA-Cl and reused FA-CL catalyst.	S17
Figure S13. Zeta potential measurements of FA-CL and reused FA-CL catalyst.	S18
Figure S14. XRD patterns of FA-CL and reused FA-CL catalyst.	S19
Figure S15. HMF yields from various saccharides over FA-CL catalyst.	S20
Figure S16. HRMS data of reaction mixture after 3 h of catalytic conversion of glucose (0.5 g) in 5 mL DT water over FA-CL catalyst.	S21
Figure S17. ¹ H-NMR spectrum of reaction mixture after 3 h of catalytic conversion of glucose (0.5 g) in 5 mL DI water over FA-CL catalyst.	S21
Figure S18. HR-TEM images and corresponding SAED patterns of (a-c) pristine clay (CL), (d-f) acid-activated FA-CL, and (g-i) reused FA-CL catalyst.	S22
Figure S19. FE-SEM images of (a) acid-activated FA-CL catalyst and (b) reused FA-CL catalyst after reaction.	S22
Table S1: Green metrics parameters for conversion of glucose to HMF using FA-CL catalyst.	S23
References	S24

Experimental Section

Materials

Natural montmorillonite clay was collected from a local source in Rajasthan, India. Formic acid (99%), D-glucose ($\geq 99\%$), D-fructose ($\geq 99\%$) were acquired from Acros Organics. Malonic acid (99%), 5-hydroxymethylfurfural (HMF, 99%), and Levulinic acid (98%) were procured from Sigma-Aldrich. Acetic acid (99%) was purchased from Qualigens. Sucrose (99%) and D-maltose monohydrate (95%) were acquired from Alfa aesar. Deionized water was prepared via Merck Millipore water system. HPLC grade solvents were used for HPLC analysis.

General Characterization

X-ray diffraction (XRD) measurements were performed using a Malvern PANalytical Empyrean diffractometer employed with Cu K α radiation ($\lambda = 1.5406 \text{ \AA}$). The samples were crushed into fine powder (approx. 100 mg) before analysis and the diffraction angle ranged from 5° to 80° with a scanning rate of $0.1^\circ/\text{s}$ and a step size of 0.02° . N $_2$ adsorption-desorption measurements were performed on Quantachrome Autosorb iQ3 instrument at 77 K to determine the specific surface area of the samples. Before analysis, the samples were degassed at 300°C under vacuum for 2 h to remove moisture or adsorbed contaminants. The specific surface areas were calculated by the Brunauer-Emmett-Teller (BET) method in the P/P_0 range of 0.05–0.25. Pore size distributions were calculated from the adsorption branch of isotherms according to the Barrett–Joyner–Halenda (BJH) method. Fourier transform infrared (FT-IR) spectra were recorded using a Bruker Alpha II FT-IR spectrometer. The samples were prepared by a halide pressing method. Samples were pre-dried, mixed with KBr at a mass ratio of (5:95 w/w ratio) and ground thoroughly. The pellets were scanned immediately after preparation under ambient conditions within a range of $400\text{--}4000 \text{ cm}^{-1}$, representing the average of 32 scans at a resolution of 4 cm^{-1} . Thermogravimetric analysis (TGA) was conducted on a PerkinElmer simultaneous thermal analyzer (STA) 6000, wherein the samples were heated from 30 to 800°C at a heating rate of $10^\circ\text{C}/\text{min}$. Energy-dispersive X-ray fluorescence spectroscopy (ED-XRF) analysis was performed on Malvern PANalytical Epsilon 4 with Ag anode target (15 W) as X-ray source. The NH $_3$ temperature programmed desorption (TPD) measurements were conducted on Altamira instruments USA (AMI-300), a chemisorption analyzer equipped with a thermal conductivity detector (TCD). Zeta potential measurements of aqueous suspensions of clays were conducted on Malvern PANalytical Zetasizer Pro where water was used as a dispersant. Solid-state MAS (magic-angle spinning) NMR spectra were recorded on a Bruker AVANCE NEO 400 MHz NMR spectrometer equipped with 4 mm CP-MAS probe. Larmor frequencies of ^1H , ^{27}Al , ^{13}C and ^{29}Si nuclei were 400.14 MHz, 104.26 MHz, 100.62 MHz and 79.50 MHz, respectively. Sample MAS frequencies were 10 kHz for the measurements. The ^1H spectra were acquired using a Hahn echo pulse sequence of $\pi/2$ and π pulses with a duration of 2.2 μs and 4.4 μs , respectively, 32 scans and a delay between scans of 15 s. ^{27}Al spectra were recorded using single pulse sequence of $\pi/2$ with duration of 1.0 μs , 400 scans and delay between scans of 5 s. ^1H - ^{13}C cross-polarization (CP) spectra were recorded using a ^1H excitation pulse of 2.2 μs and contact time of 2.5 ms, 3000 scans with delay between scans of 5 s. ^{29}Si spectra were recorded using single pulse sequence of $\pi/2$ with duration of 3.84 μs , 350 scans and delay between scans of 120 s. The shift axis in all the spectra was referenced using an external reference of adamantane. Pyridine-adsorbed infrared (IR) spectra were obtained to differentiate B and L acid sites on the catalyst using a PerkinElmer FT-IR spectrometer, operating at a resolution of 4 cm^{-1} and averaging 32 scans. Samples were prepared as self-supporting pellets (13 mm diameter, 40 mg) and prior to measurement, the pellets were dehydrated by heating under vacuum at 350°C for 1 hour. Subsequently, pyridine vapor was then introduced into the cell at room temperature for 10 min until adsorption equilibrium was achieved. Further desorption

steps were carried out by evacuating the cell at different temperatures ranging from 150 to 350 °C for 10 minutes each, followed by spectral acquisition. The concentrations of Bronsted (B) and Lewis (L) acid sites, along with their B/L ratios, were calculated by the integrated areas of the characteristic pyridine adsorption peaks following desorption at 150 °C, by using the molar extinction coefficient method, proposed by Emeis. These are the following expressions for quantification as reported in literature²:

$$C_L = K_L \times A_{1450} = \frac{\pi}{\text{IMEC}_L} \times \left(\frac{r^2}{w}\right) \times A_{1450} \text{ and}$$

$$C_B = K_B \times A_{1540} = \frac{\pi}{\text{IMEC}_B} \times \left(\frac{r^2}{w}\right) \times A_{1540}$$

where C_L and C_B are concentrations of Lewis acid sites (LAS) and Bronsted acid sites (BAS) in $\mu\text{mol g}^{-1}$, K_L and K_B are molar extinction constants for LAS and BAS, A_{1450} and A_{1540} are integrated areas of bands at 1450 and 1540 cm^{-1} . IMEC_L and IMEC_B are integration molar extinction coefficients, which are 2.22 and 1.67 $\text{cm } \mu\text{mol}^{-1}$ of LAS and BAS, r is the wafer radius in cm, and w is the wafer weight in g, respectively.

Catalysts Preparation

A natural montmorillonite clay (Montmorillonite-15A) obtained from Rajasthan, India, was used in this study, and its mineralogical identity was confirmed by X-ray diffraction using the ICDD reference pattern (PDF No. 00-013-0135). The clay was purified following a procedure as mentioned earlier.³ Briefly, the clay was treated (ball-milled), sieved, washed thoroughly with deionized water three times, kept for sedimentation for 5 h, and dried in an oven at 100 °C overnight. The acid-treated clay was prepared using different organic acids (formic acid (FA), acetic acid (AA), and malonic acid (MA)), respectively. In a typical procedure, 1g of clay was stirred with 10 mmol of organic acid in 10 mL deionized water, in a closed boiling flask at 80 °C, for 2 h. After acid treatment, the mixture was transferred to a centrifuge tube, and the treated clay was separated by centrifugation at 12000 rpm for 10 minutes, washed thoroughly with deionized water (until neutral pH) to remove the unreacted acid (checked the pH of supernatant), then dried overnight at 80 °C and ground in mortar pestle. The dried clay was calcinated in the muffle furnace under static air at 500 °C for 5 h with a ramping rate of 10 °C min^{-1} . The clays are labelled as acid-CL, where CL stands for clay abbreviated as FA-CL (formic acid-treated clay), AA-CL (acetic acid-treated clay), and MA-CL (malonic acid-treated clay).

Catalytic conversion

All the catalytic reactions were conducted in a sealed pressure tube heated in a temperature-controlled oil bath on a digital stirring hot plate equipped with a thermocouple. In a typical experiment, 0.5 g of reactant, 0.05 g of catalyst (reactant-to-catalyst weight ratio of 10:1) and 5 mL of water were added into the pressure tube and then sealed properly. The reaction mixture was stirred at 500 rpm at various temperatures for a given reaction time. The reaction progress was monitored at fixed time intervals using thin-layer chromatography (TLC) with a 9:1 $\text{CHCl}_3/\text{CH}_3\text{OH}$ mobile phase. After the target reaction time was reached, the reaction vessel was immersed in ice-cold water to quench the reaction. The reaction mixture was filtered through a 0.25 μm filter membrane and subsequently used for product analysis. For purity analysis, the HMF was extracted from the reaction mixture through liquid-liquid extraction by using ethyl acetate (5×20 mL) and brine (sat. NaCl) solution. Then collected organic layer was dried upon anhydrous sodium sulphate and evaporated through a rotary evaporator (water bath temperature 40 °C and rotation speed 70 rpm). The crude extract was purified by silica-gel column chromatography (60-120 mesh) by using hexane: ethyl acetate as eluent starting from 9:1 ratio and

eluting HMF at 7:3. The HMF purity was checked by HPLC and ¹H NMR spectroscopy. All reactions were conducted in triplicate, and the results are reported as mean ± standard deviation (S.D.), with error bars representing the variability among replicates.

Product analysis

The concentrations of glucose, fructose, HMF, and levulinic acid were evaluated by High Performance Liquid Chromatography (HPLC). The analysis was performed on the Thermo Scientific Vanquish HPLC system equipped with a diode-array detector (DAD) and refractive index (RI) detector. HMF and LA quantification was carried out on a C18 column using the DAD at a detection wavelength of 284 nm under isocratic elution with methanol–water (20:80, v/v) as the mobile phase, a flow rate of 0.8 mL/min, and an injection volume of 10 μL. Quantification of sugars (glucose and fructose) was performed using an RI detector with a SUPELCOSIL LC-NH2 column at 30 °C, employing an acetonitrile–water mixture (75:25, v/v) as the mobile phase at a flow rate of 0.7 mL/min. The glucose conversion, product yield, and carbon balance were calculated by using following equations:

$$\text{Glucose conversion (mol\%)} = \frac{\text{moles of glucose reacted}}{\text{moles of initial glucose}} \times 100$$

$$\text{Product yield (mol\%)} = \frac{\text{moles of product formed}}{\text{moles of initial glucose}} \times 100$$

$$\text{Carbon balance (\%)} = \frac{\text{moles of } C_{\text{product}} + \text{moles of } C_{\text{unreacted glucose}}}{\text{moles of } C_{\text{initial glucose}}} \times 100$$

Catalyst recyclability

The recyclability of the FA-CL catalyst was evaluated over ten successive catalytic cycles. In a typical run, 1 g of glucose, 100 mg of FA-CL (10% w/w), 10 mL of DI water were added to a pressure tube with magnetic bead and placed in a preheated oil bath at 145 °C under constant stirring for 6 h. After 6 h, the reaction mixture was cooled down and the catalyst was separated using centrifugation. The centrifuge was performed at 12000 rpm for 10 min and the supernatant was collected for further analysis. The solid catalyst was washed with DI water (3×10 mL) followed by ethanol (10 mL each time) and dried in oven at 120 °C overnight to activate the catalyst for further cycles. The recovered catalyst was reused for up to ten consecutive runs under identical reaction conditions.

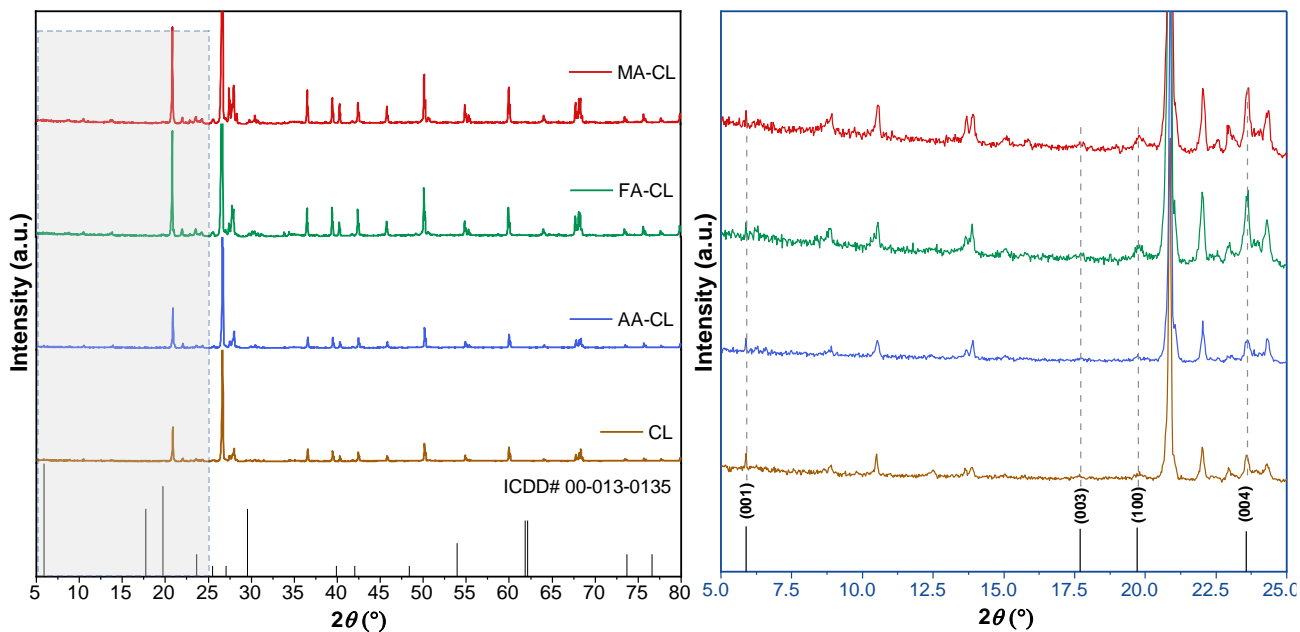


Figure S1. XRD patterns of the untreated clay (CL) and after activation with acetic acid (AA-CL), formic acid (FA-CL), and malonic acid (MA-CL). The diffraction patterns displayed the characteristic reflections of montmorillonite with some quartz content, while the sharpening and increased reflections after acid treatment are attributed to the removal of amorphous impurities and preservation of the layered crystalline structure.

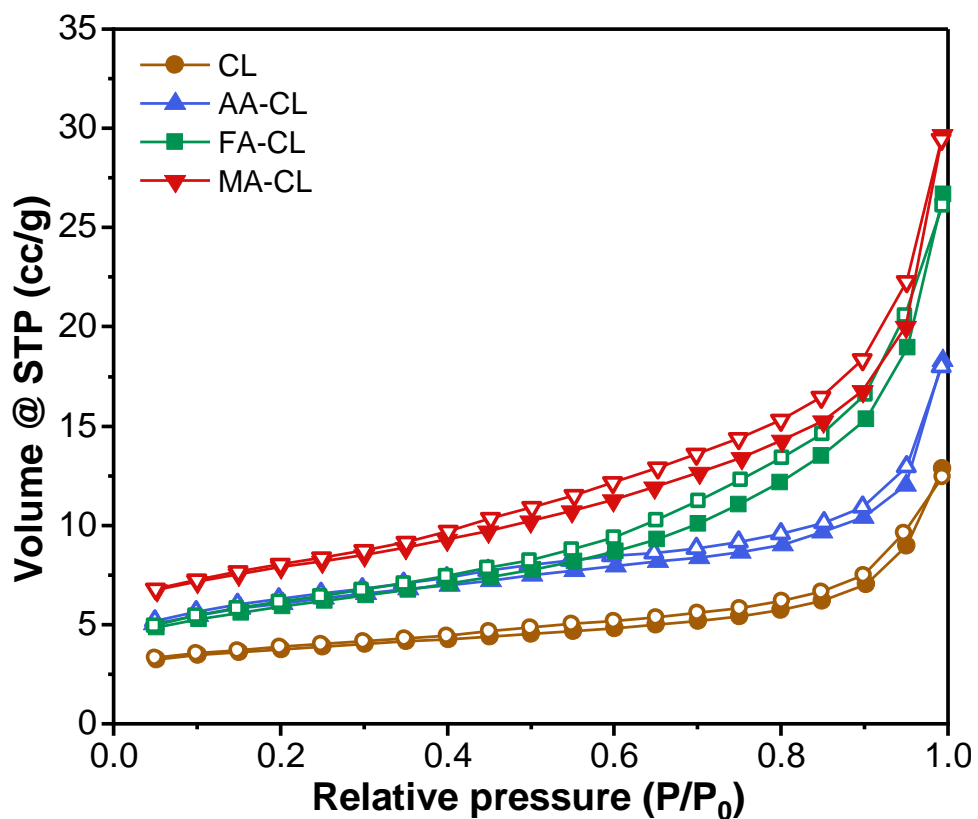


Figure S2. N₂ adsorption-desorption isotherms of CL, AA-CL, FA-CL, and MA-CL in the relative pressure range 0.0—1.0. The clay represents a typical type-IV isotherm with H3 hysteresis loop representing the particles forming slit-shaped pores upon acid activation due to generation of mesoporosity.

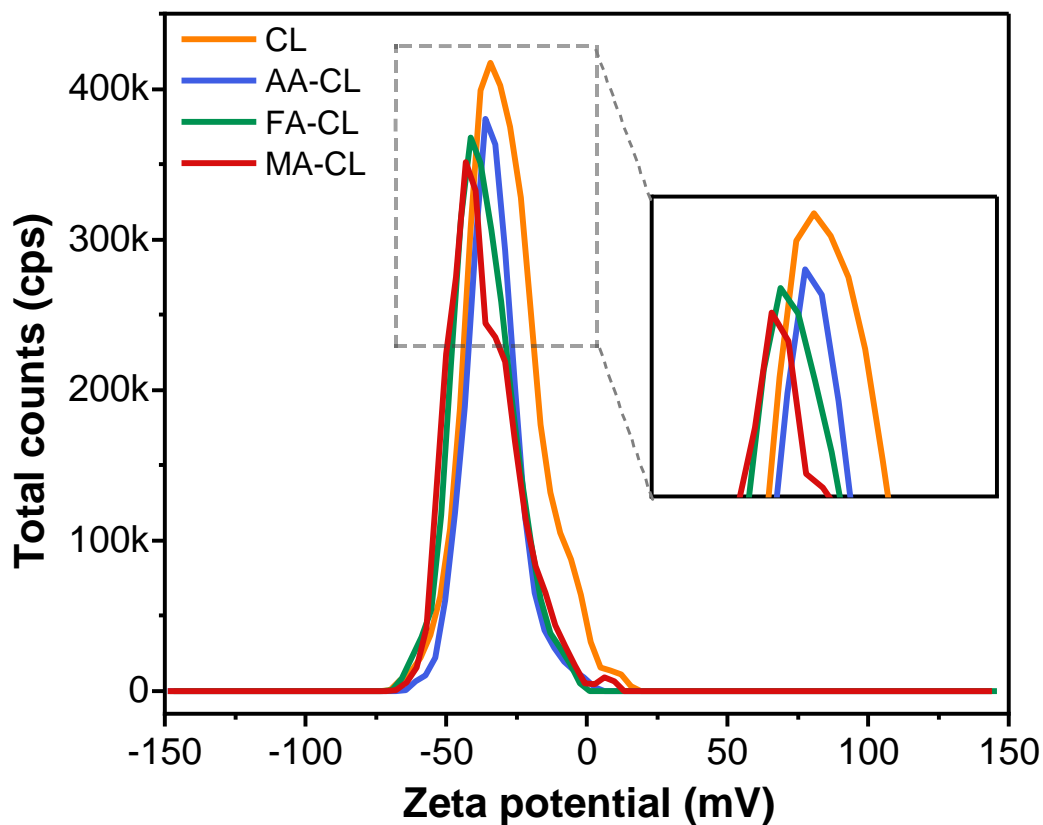


Figure S3. Zeta potential measurements of CL, AA-CL, FA-CL, and MA-CL. Acid treatment of clay leads to leaching of aluminium ions from octahedral layer which introduces the new layer with terminal hydroxy groups, results in increase of Brønsted acidity. More the layers, more will be the negative charge (terminal -OH groups) and hence more negative will be the zeta potential. The order of zeta potential from most -ve to +ve as follows- MA-CL>FA-CL>AA-CL>CL.

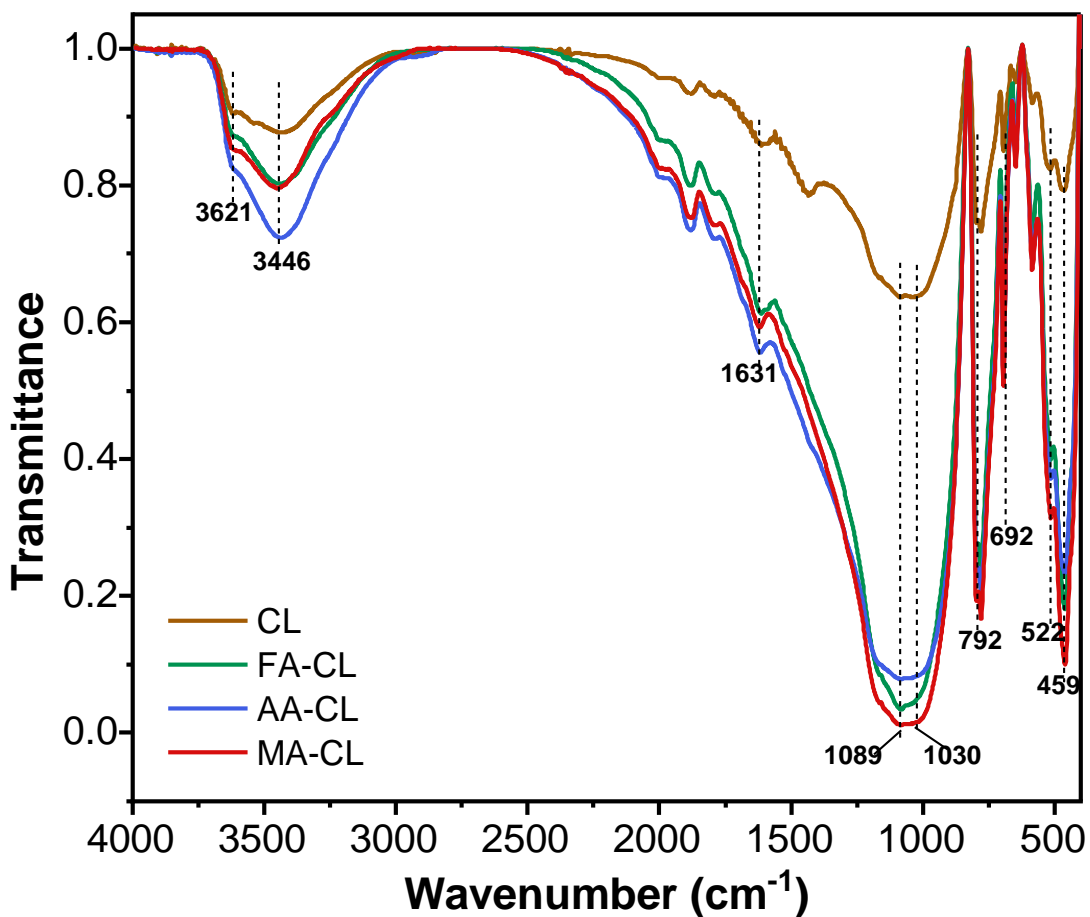


Figure S4. FTIR spectra of CL, AA-CL, FA-CL, MA-CL. The broad and intense Si-O stretching bands at 1030 (in-plane) and 1089 cm^{-1} (out-of-plane). The peak at 792 cm^{-1} assigned to the cristobalite impurity. Sharp peak at 692 cm^{-1} corresponds to the quartz. Al-O-Si and Si-O-Si deformations at 522 and 459 cm^{-1} . The -OH stretching band at 3621 cm^{-1} attributed to the structural hydroxy groups while a broad -OH stretching band at 3446 cm^{-1} corresponds to adsorbed water molecules with -OH bending vibration at 1631 cm^{-1} . The characteristic Si-O stretching band at 1030 cm^{-1} increases with acid treatment of clay.

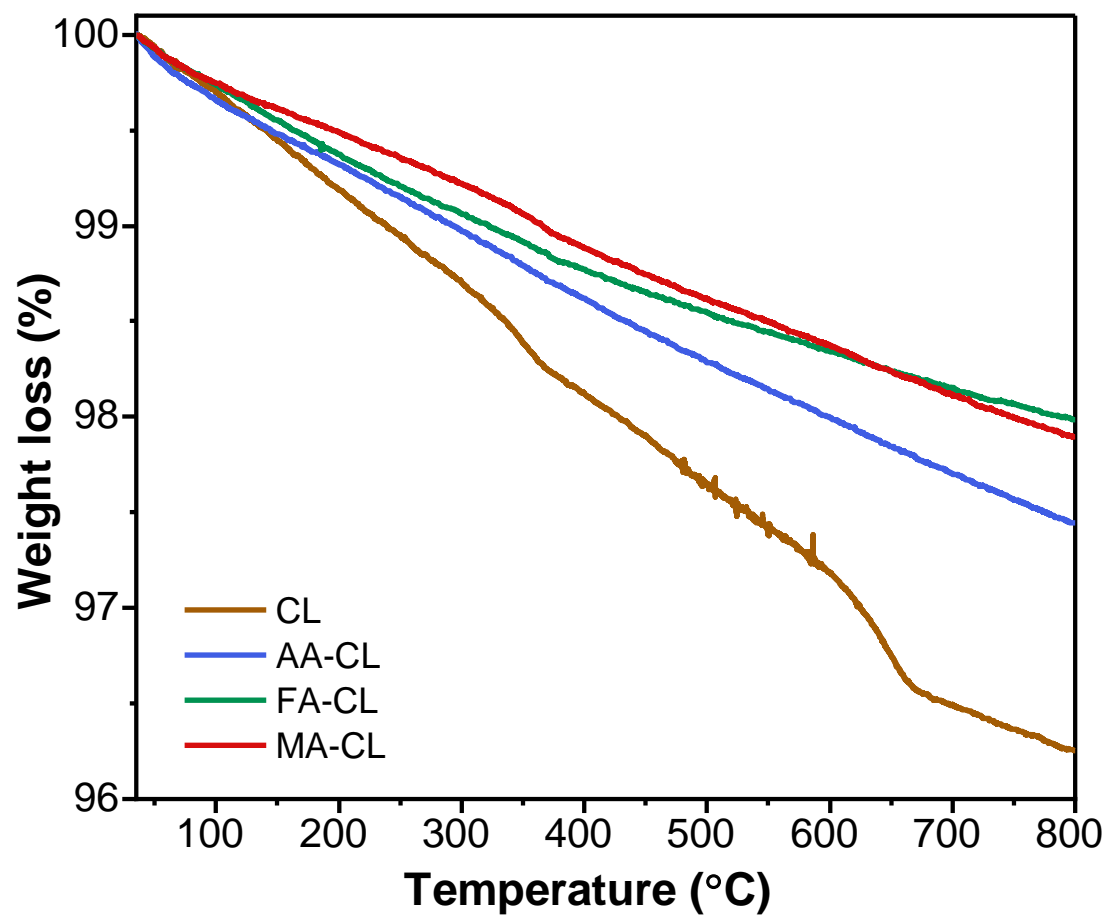


Figure S5. TGA profiles of CL, AA-CL, FA-CL, and MA-CL. The initial mass loss attributed to physically adsorbed water molecules on the clay surface and later dehydroxylation of structural -OH groups at higher temperature. The treatment of clay with organic acids provides additional stability to lamellar structure of clay.

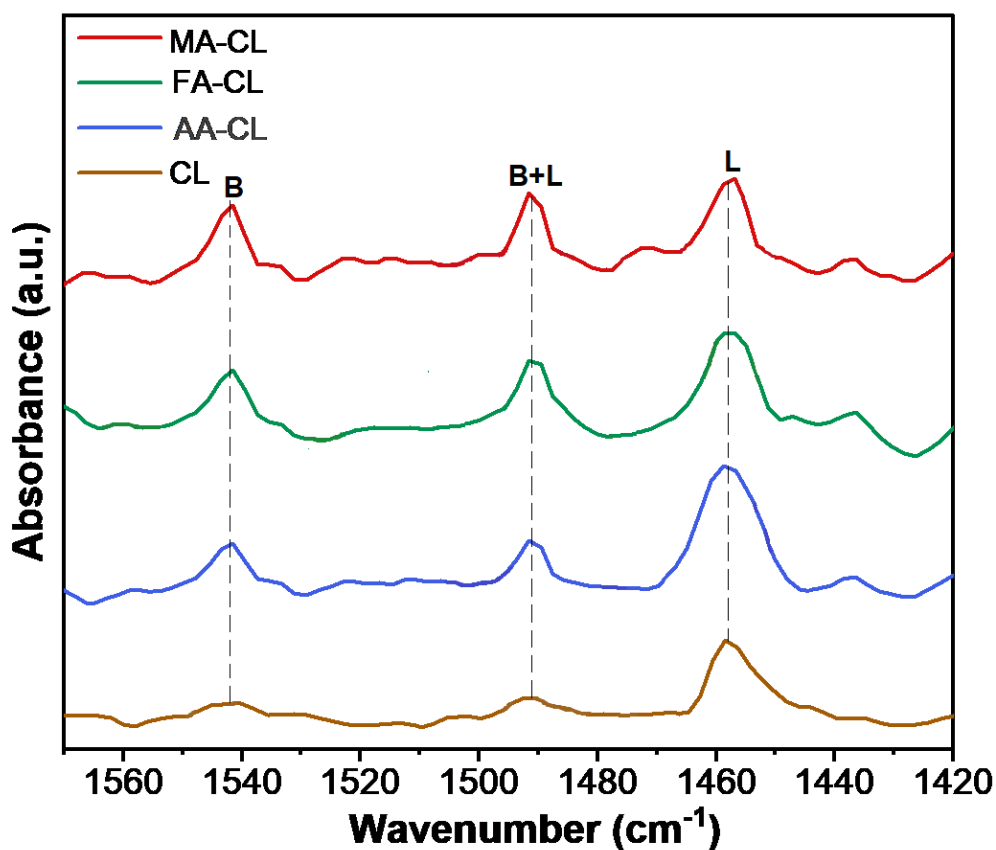


Figure S6. Pyridine-FTIR spectra of CL, AA-CL, FA-CL, MA-CL. The two absorption bands at 1445 cm^{-1} and 1650 cm^{-1} related to the Lewis acid sites while the band at 1540 cm^{-1} attributed to Brønsted acid sites. The absorption band at 1490 cm^{-1} corresponds to the pyridine molecules adsorbed at both Brønsted and Lewis acid sites. In clay, only Lewis acid sites are present while after the treatment of clay with acetic acid, Brønsted acid sites are introduced due to the presence of terminal hydroxy groups due to the formation of new layers of clay.

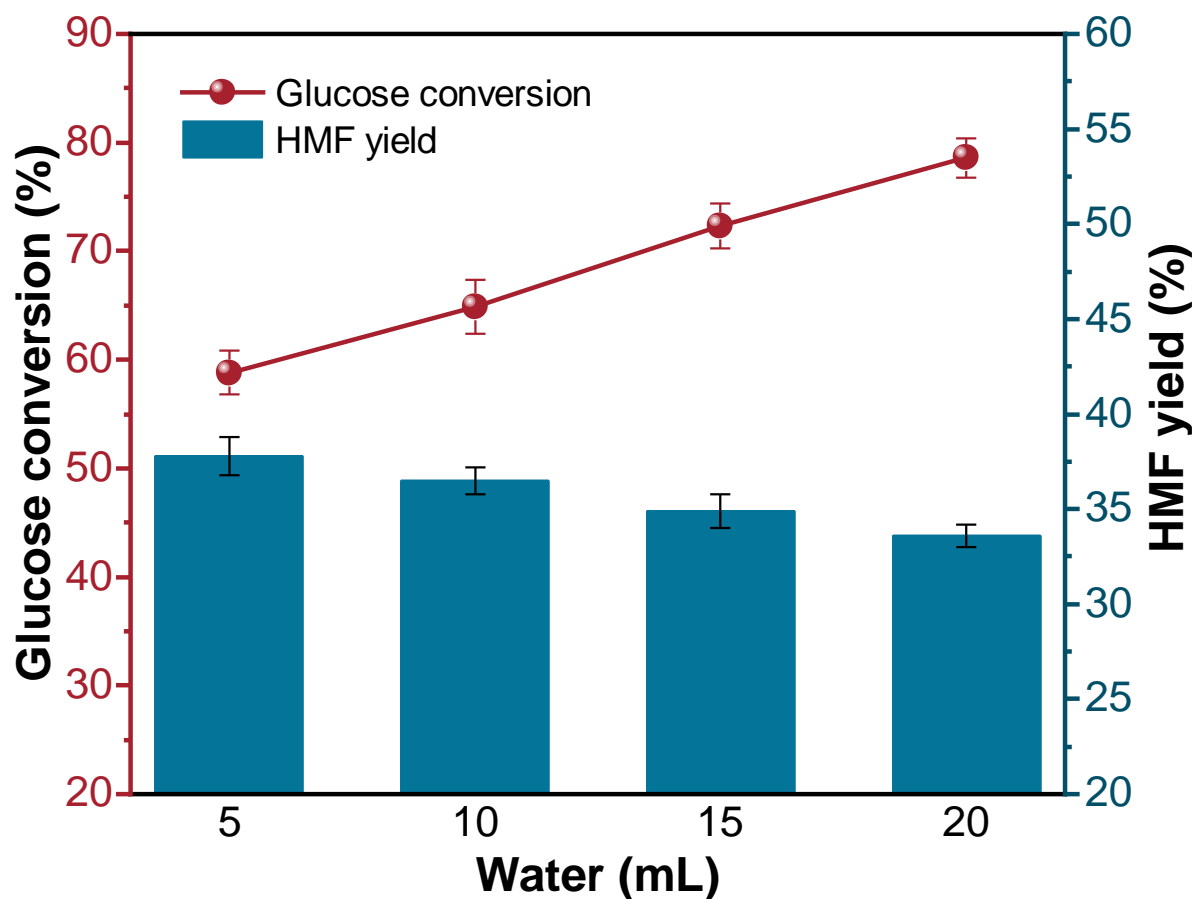


Figure S7. Effect of solvent amount on glucose conversion and HMF yield over FA-CL catalyst. Reaction conditions: 2.75 mmol of glucose, FA-CL (10 % w/w of glucose) were added into a x mL of DI water at 145 °C under continuous stirring for 3 h. The symbols and bars represent experimental values and error bars denote the standard deviation values from triplicate experiments (n = 3).

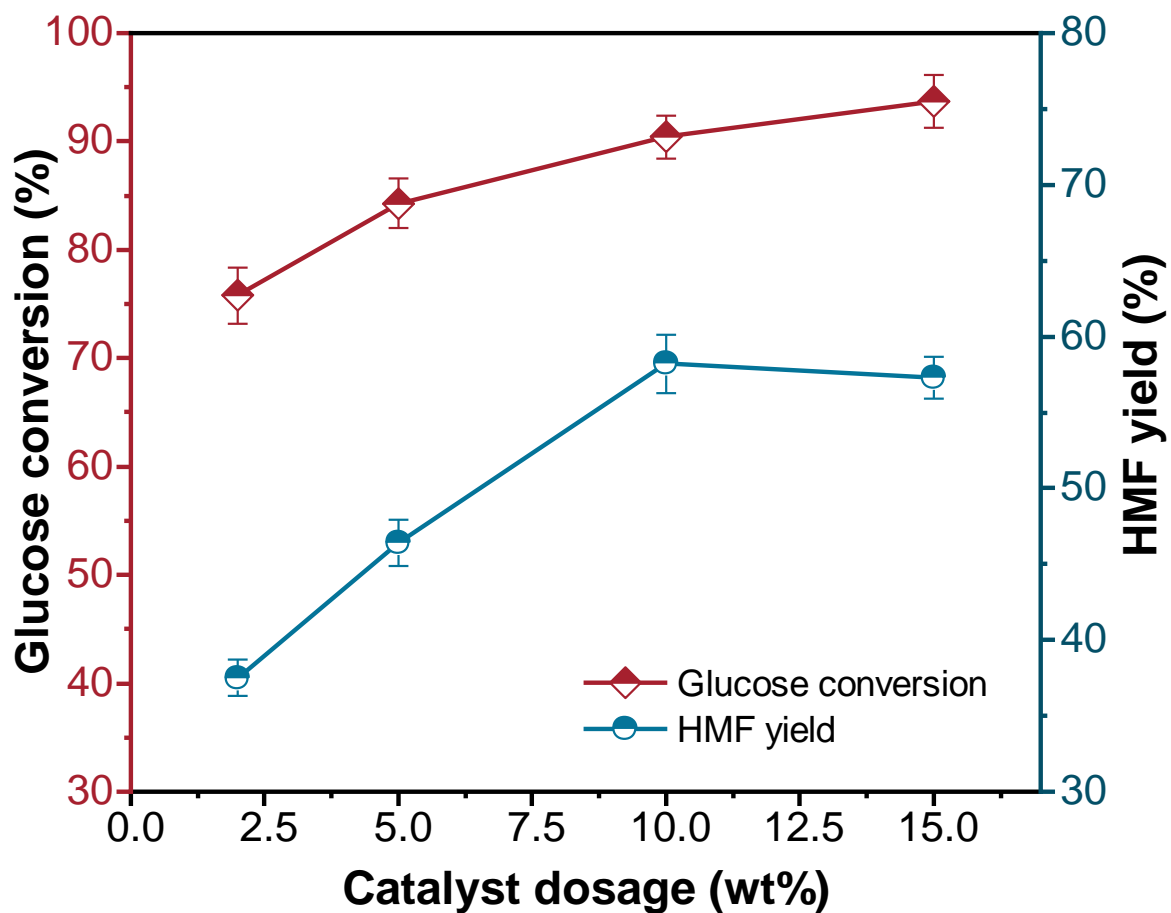


Figure S8. Effect of catalyst dosage on glucose conversion and HMF yield over FA-CL catalyst. Reaction conditions: 2.75 mmol of glucose, FA-CL (2, 5, 10, and 15 % w/w of glucose) were added into a 5 mL of DI water at 145 °C under continuous stirring for 6 h. The symbols represent experimental values and error bars denote the standard deviation values from triplicate experiments (n = 3).

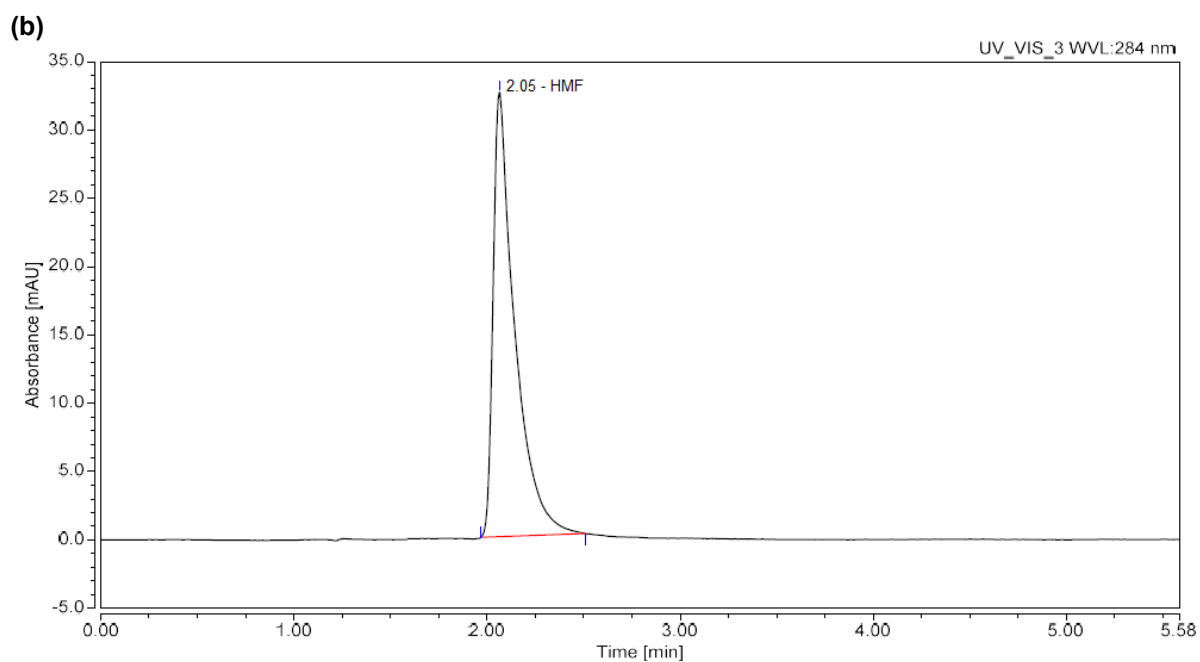
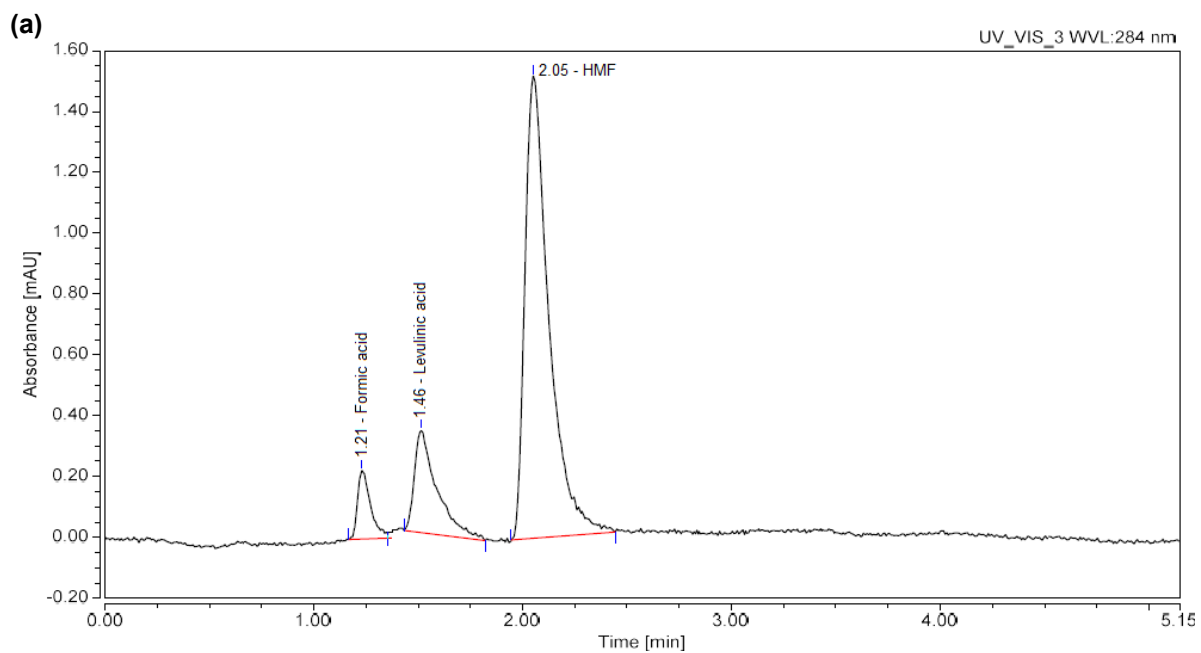


Figure S9. (a) HPLC chromatogram of crude product after 6 h of catalytic conversion of glucose over FA-CL catalyst. (b) HPLC chromatogram of purified HMF. (C18 column, DAD detector, λ 284 nm, isocratic methanol–water (20:80, v/v) mobile phase)

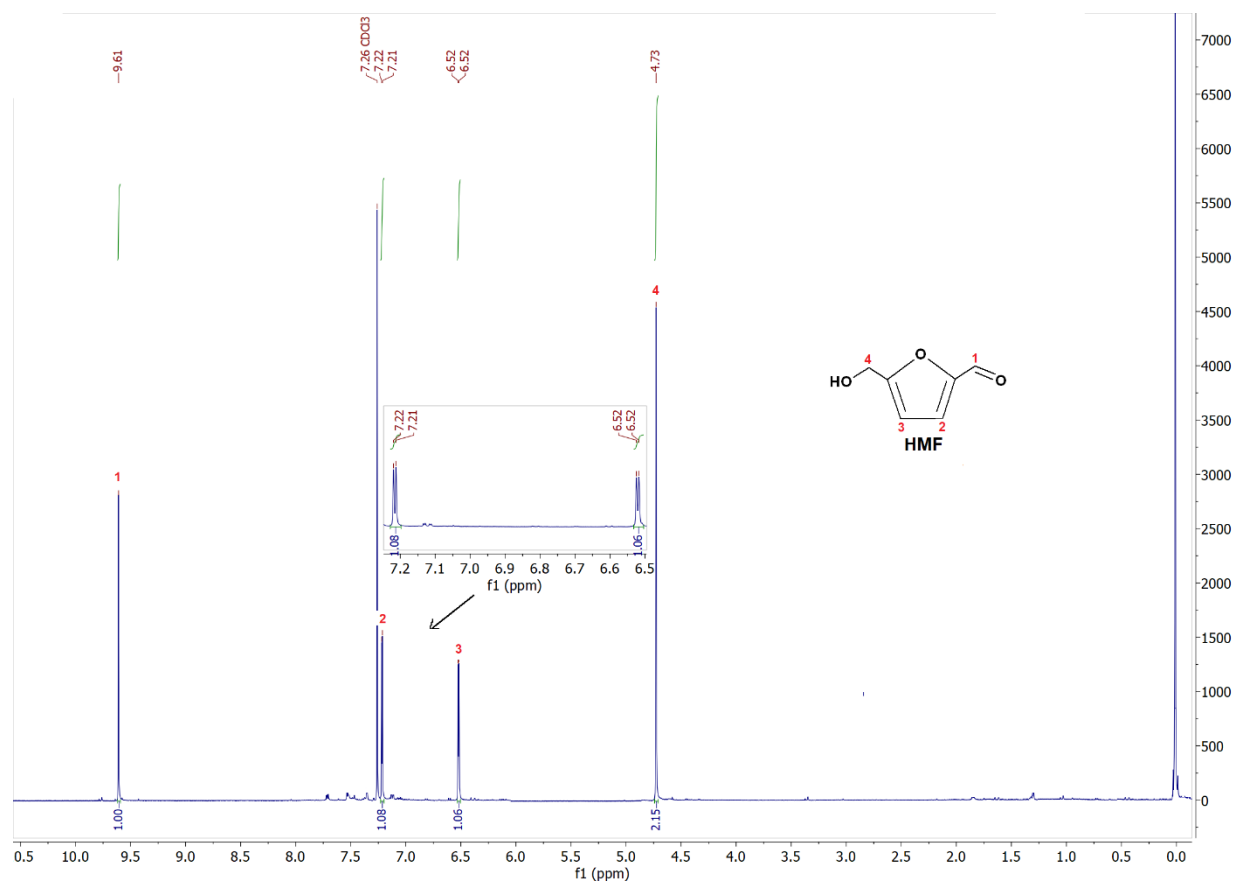


Figure S10. ¹H-NMR spectrum of purified HMF from crude product of catalytic conversion of glucose (0.5 g) in 5 mL DI water using FA-CL. ¹H NMR (500 MHz, CDCl₃) δ 9.61 (s, 1H; aldehyde-H), 7.22-7.21 (d, *J* = 5 Hz, 1H; furan-H), 6.53-6.52 (d, *J* = 5 Hz, 1H; furan-H), 4.73 (s, 2H; CH₂-OH).

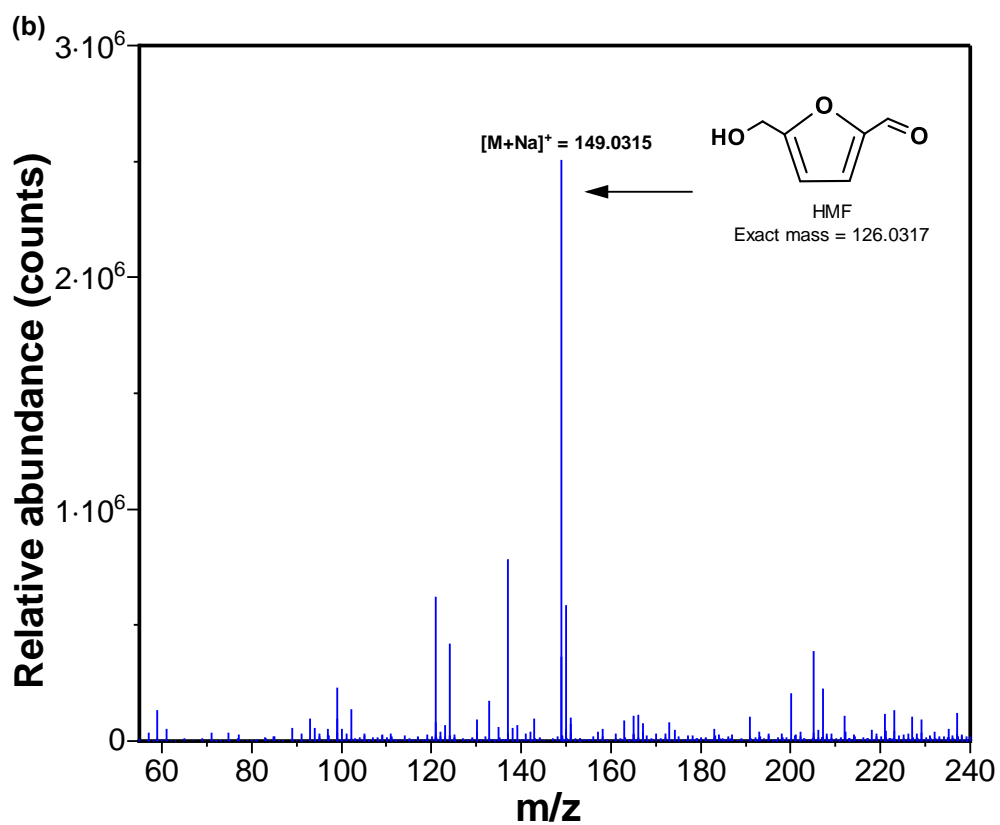
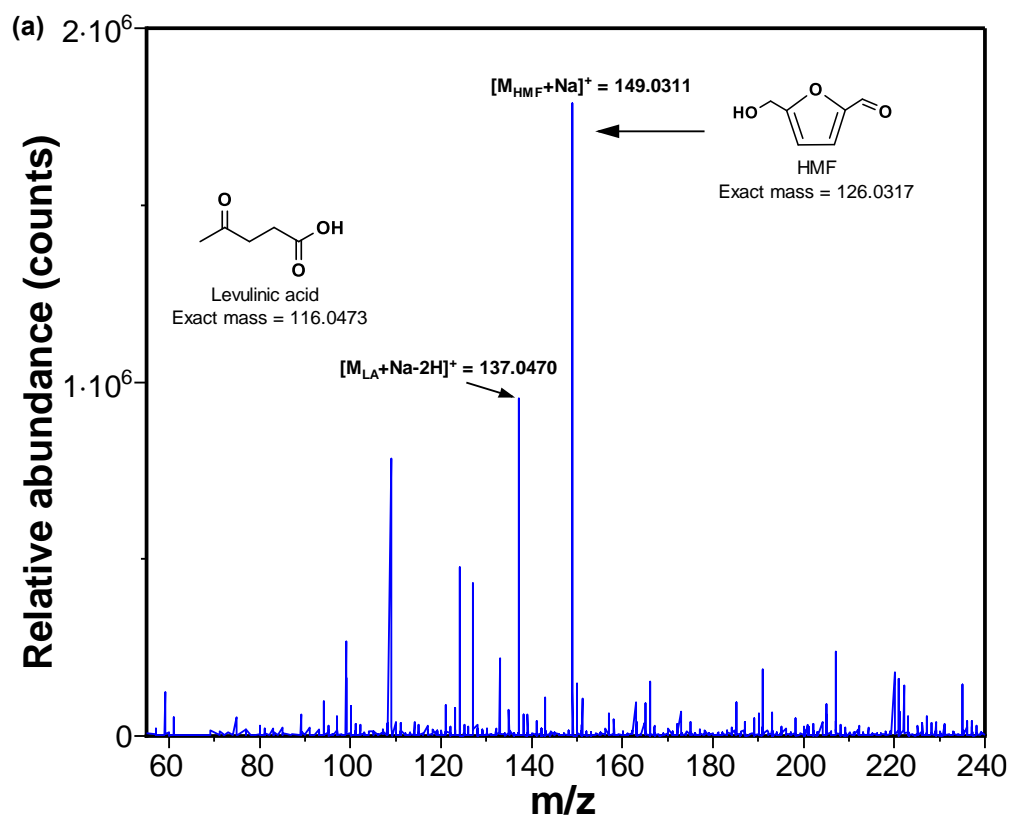


Figure S11. HRMS data of (a) crude product and (b) purified HMF after 6 h of catalytic conversion of glucose over FA-CL catalyst.

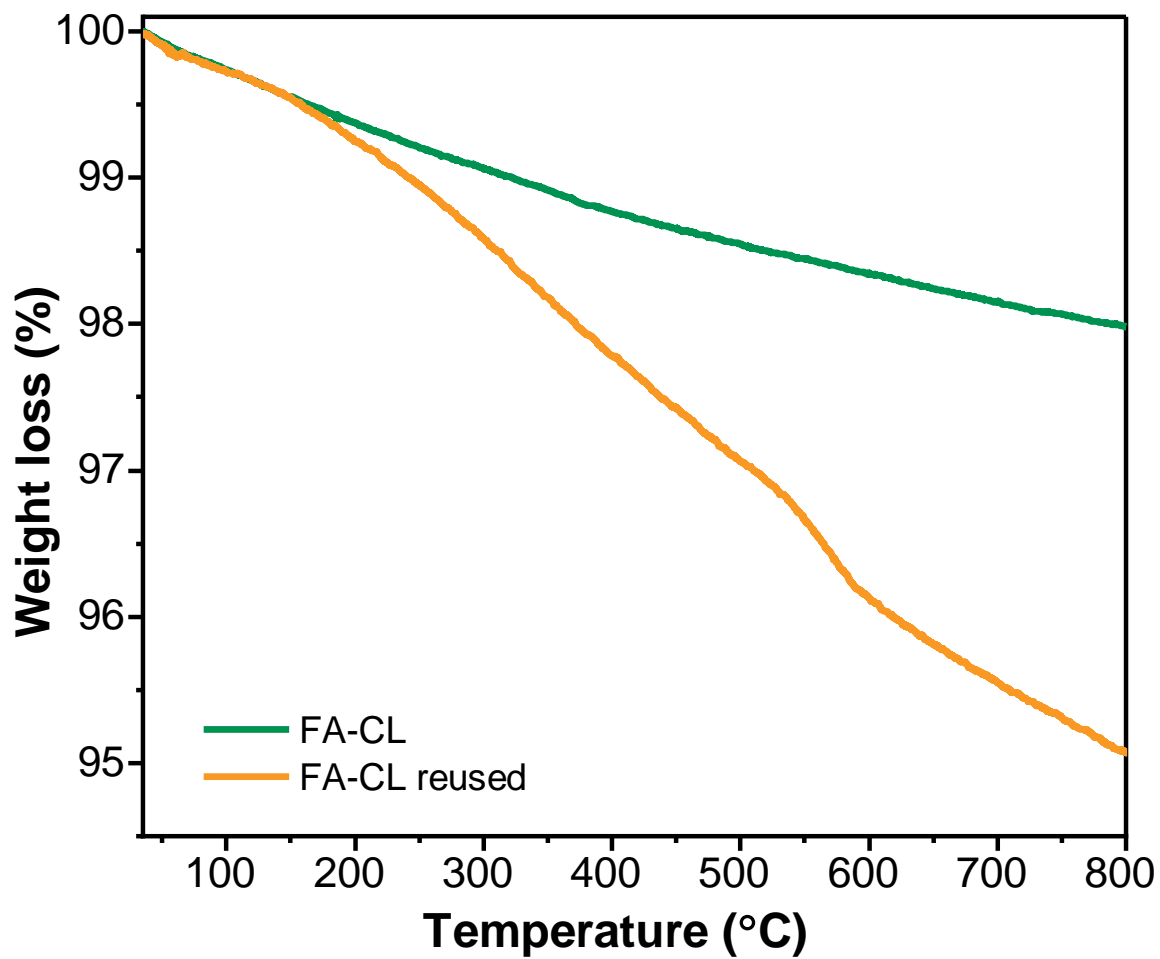


Figure S12. TGA of FA-Cl and reused FA-CL catalyst. The thermal stability of the reused FA-CL catalyst decreases due to the deposition of carbonaceous material on the catalyst's surface.

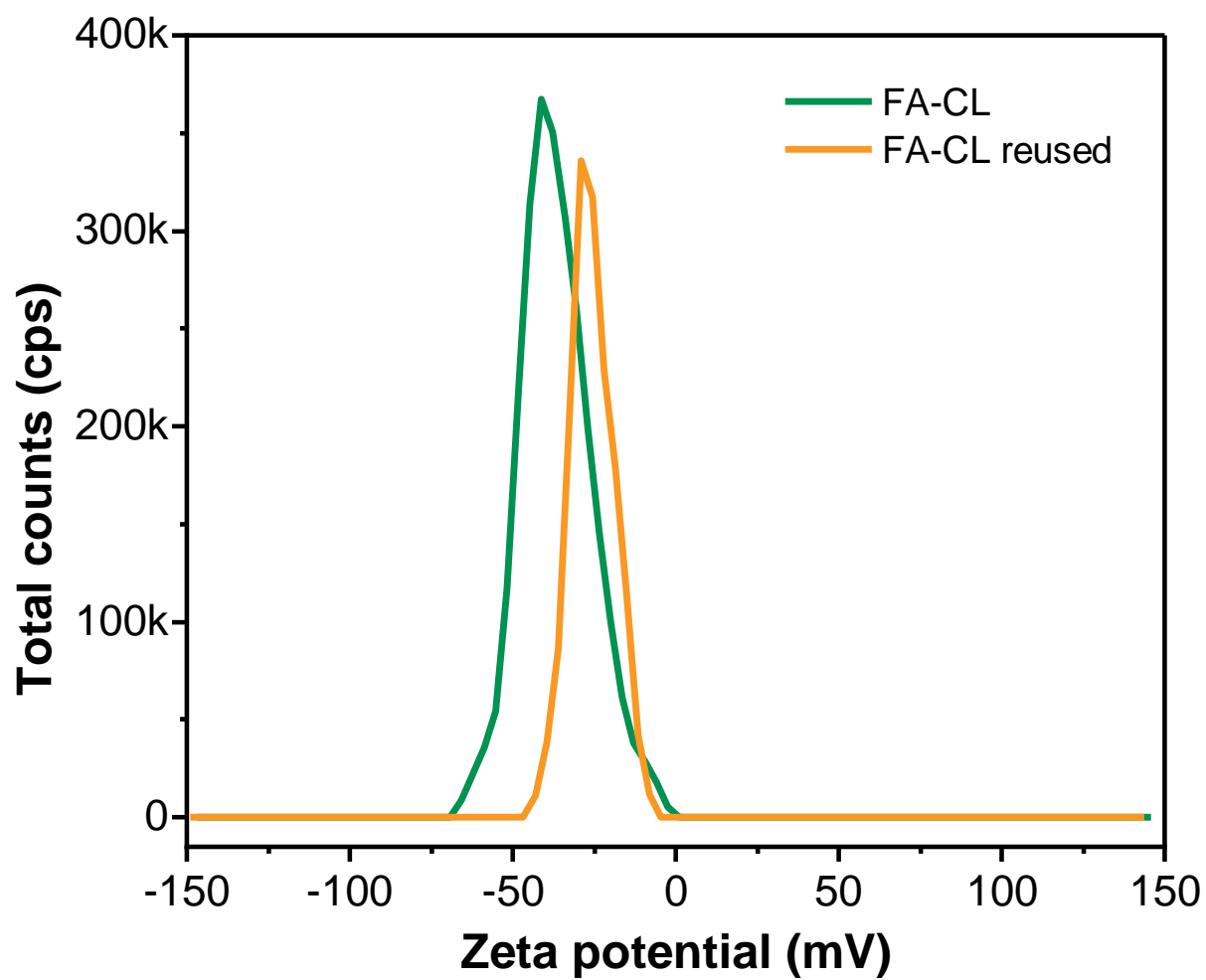


Figure S13. Zeta potential measurements of FA-CL and reused FA-CL catalyst. The highly charged surface of FA-CL due to deprotonatable silanol groups while reused FA-CL have lower zeta potential due to adsorbed molecules on the surface during catalytic conversion.

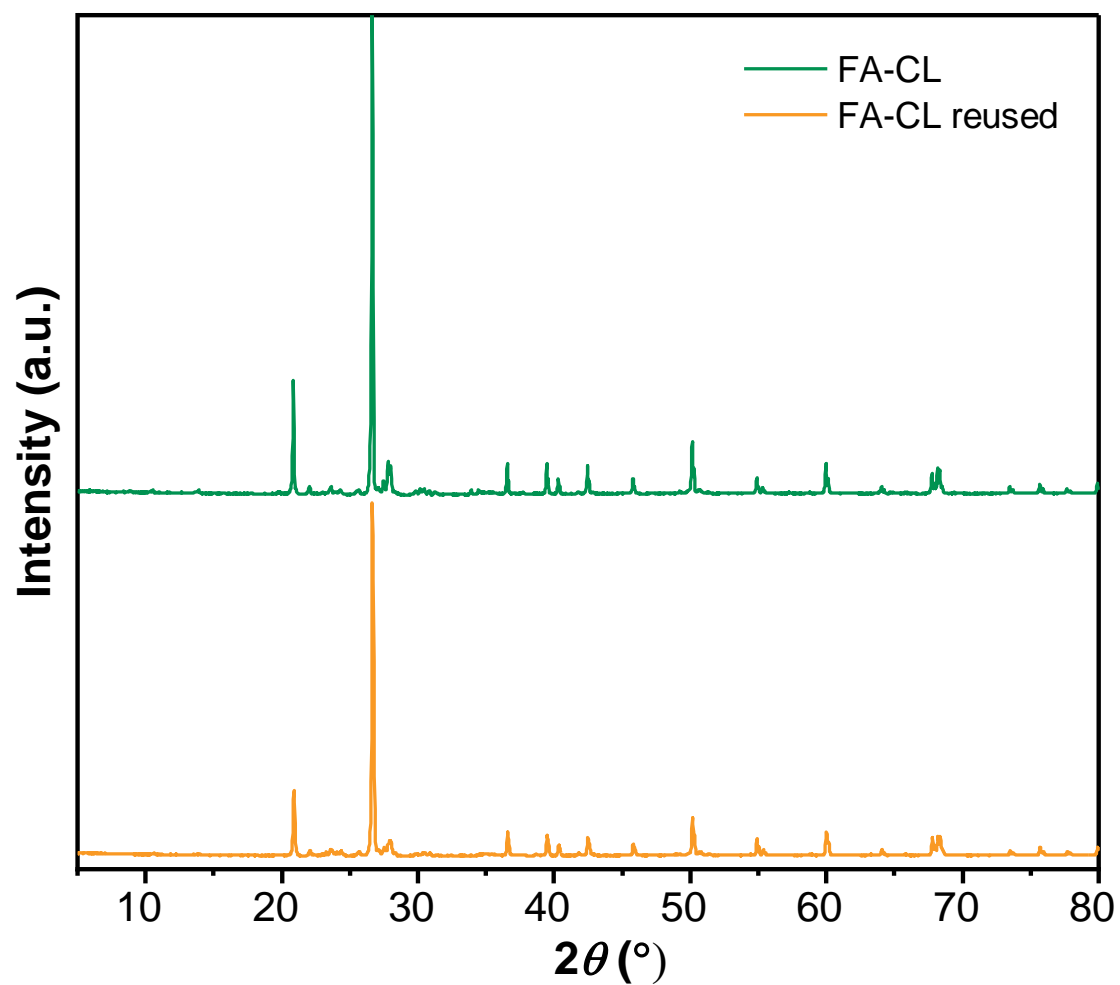


Figure S14. XRD patterns of FA-CL and reused FA-CL catalyst. The crystalline structure of clay preserved after catalytic conversion.

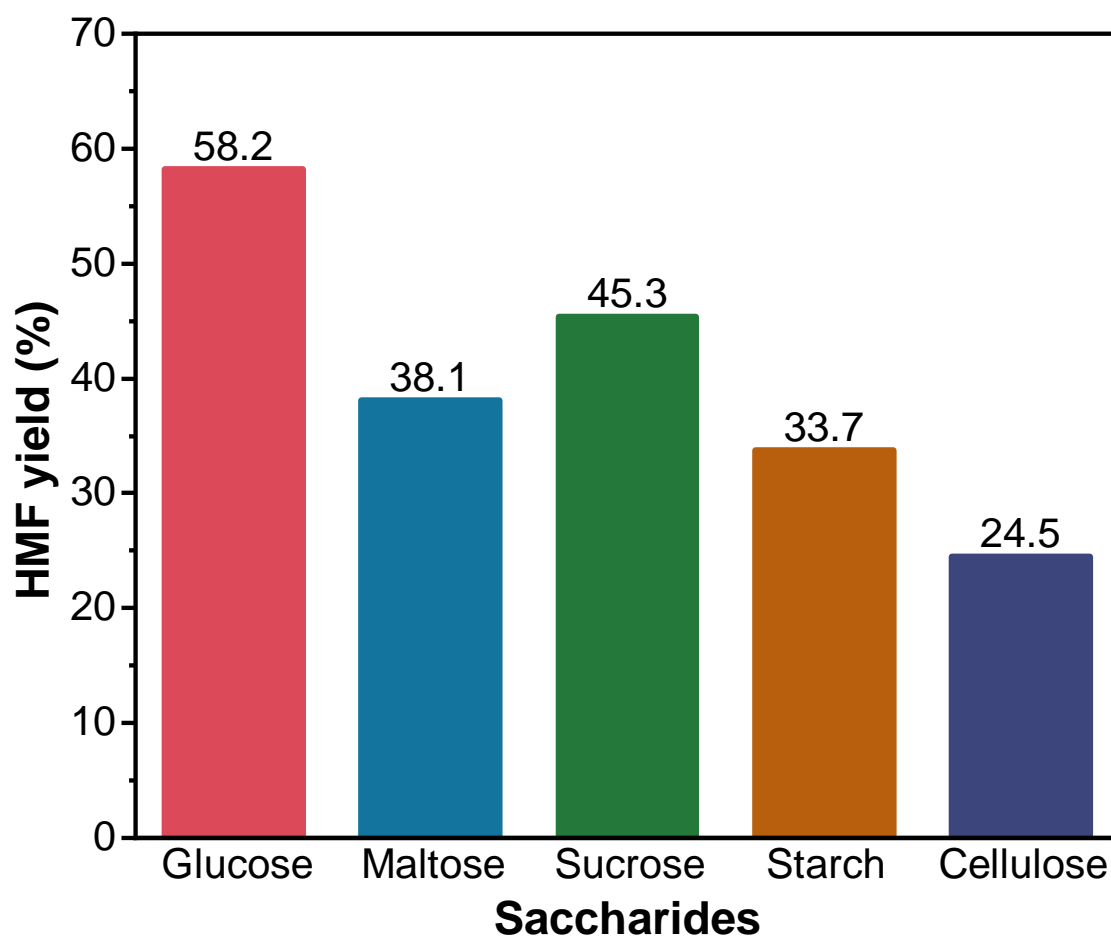


Figure S15. HMF yields from various saccharides over FA-CL catalyst. Reaction conditions: 2.75 mmol of saccharides, FA-CL (10 % w/w of substrate) were added into a 5 mL of DI water at 145 °C under continuous stirring for 6 h.

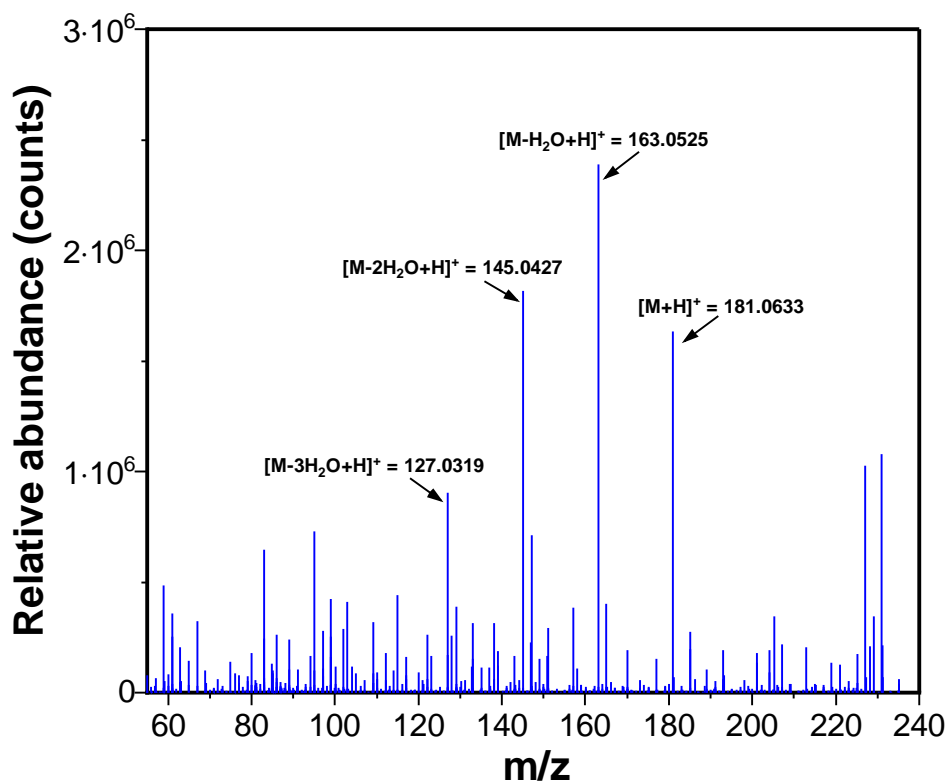


Figure S16. HRMS data of reaction mixture after 3 h of catalytic conversion of glucose (0.5 g) in 5 mL DT water over FA-CL catalyst.

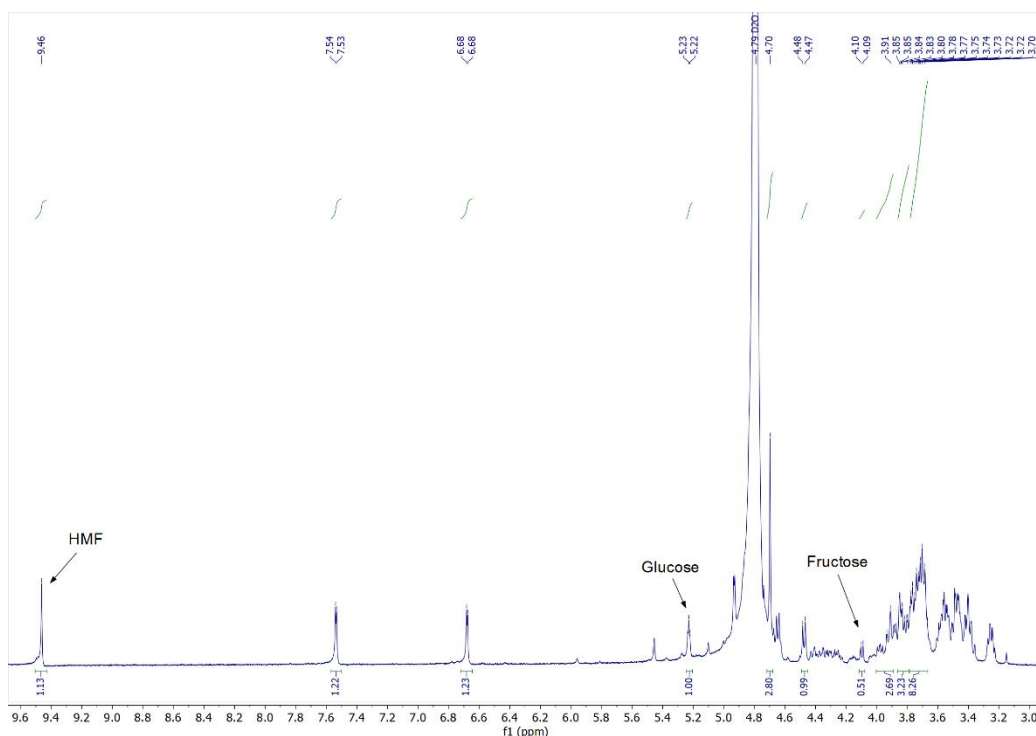


Figure S17. $^1\text{H-NMR}$ spectrum of reaction mixture after 3 h of catalytic conversion of glucose (0.5 g) in 5 mL DI water over FA-CL. The anomeric proton (H-1) of glucose exhibits the doublet at 5.19-5.20 ppm while the C-2 proton (H-2) of fructose exhibits the doublet at 4.09-4.10 ppm. The decrease of the glucose anomeric H-1 signal (5.20 ppm) and simultaneous appearance of fructose H-2 signal (4.09 ppm) confirms the formation of fructose as an intermediate.

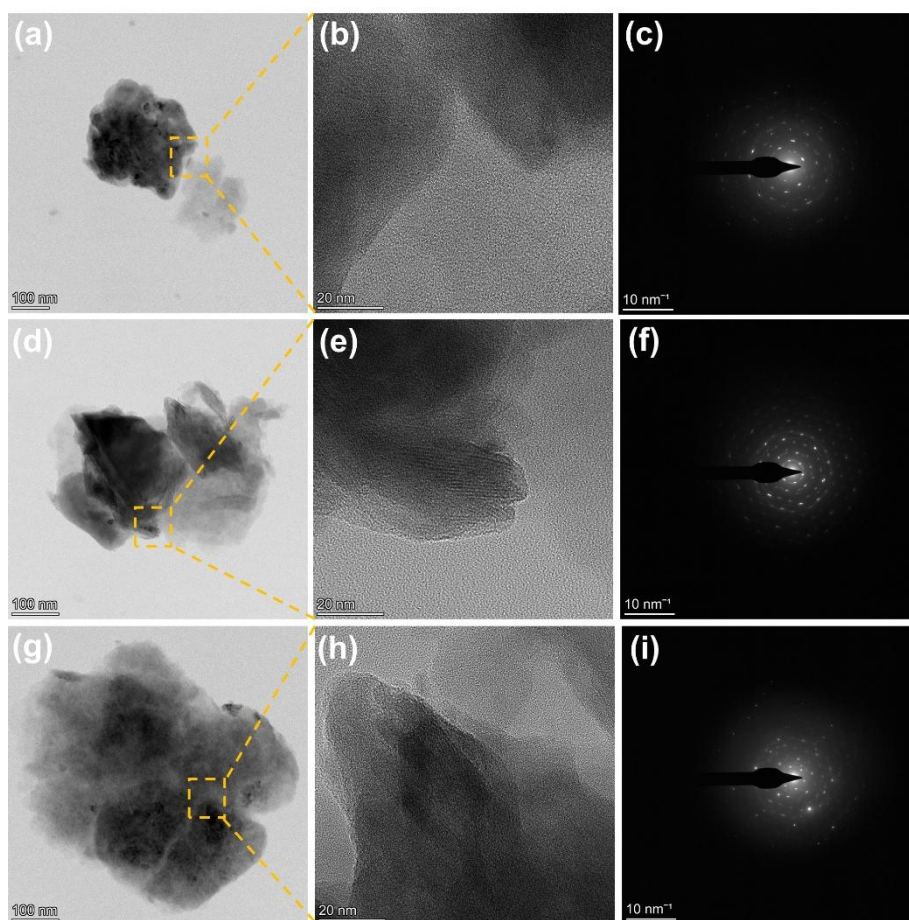


Figure S18. HR-TEM images and corresponding SAED patterns of (a-c) pristine clay (CL), (d-f) acid-activated FA-CL, and (g-i) reused FA-CL catalyst. The images show retention of the layered clay microstructure after acid activation and recycling. Corresponding SAED patterns confirm preservation of the crystalline framework before and after catalytic use.

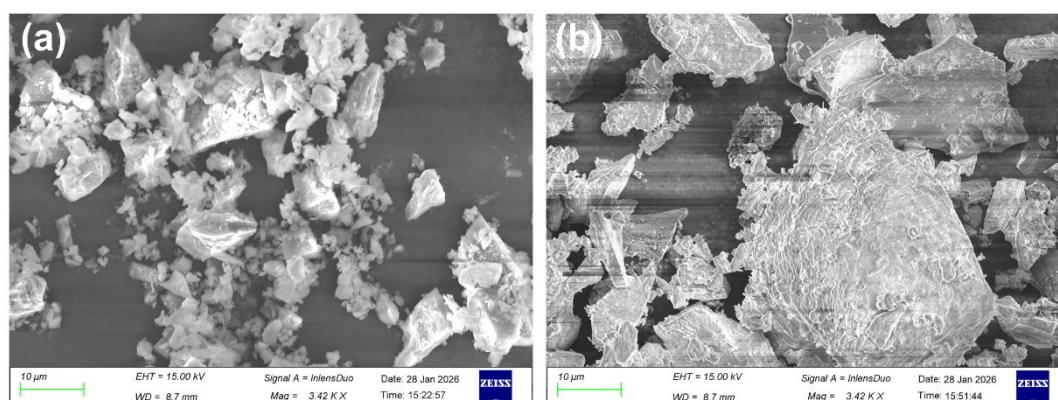


Figure S19. FE-SEM images of (a) acid-activated FA-CL catalyst and (b) reused FA-CL catalyst after reaction. The images showed a layered and lamellar platelet morphology, indicating preservation of surface structure upon recycling.

Green metrics calculation

- **Carbon efficiency**

Formula:
$$\text{Carbon efficiency (\%)} = \frac{\text{mass of carbon in product}}{\text{mass of carbon in reactant}} \times 100$$

This simplifies:

$$\text{Carbon efficiency (\%)} = \frac{\text{HMF yield (\%)}}{\text{Glucose conversion (\%)}} \times 100$$

At optimized reaction conditions:

$$\text{Carbon efficiency (\%)} = \frac{58.2}{90.4} \times 100 = \mathbf{64.4\%}$$

- **Environmental factor (*E*-factor)**

Formula:
$$E\text{-factor} = \frac{\text{mass of waste}}{\text{mass of product}}$$

$$\text{Total mass of waste} = \text{mass of reactant} - \text{mass of product}$$

$$\text{Total mass of waste} = \text{mass of glucose (fed)} - \text{mass of HMF produced}$$

$$\text{Total mass of waste} = 0.5 \text{ g} - 0.204 \text{ g} = 0.296 \text{ g}$$

$$E\text{-factor} = \frac{0.296 \text{ g}}{0.204 \text{ g}} = \mathbf{1.45}$$

- **Atom economy**

Formula:
$$\text{Atom economy (\%)} = \frac{\text{Molecular weight}_{\text{product}}}{\text{Molecular weight}_{\text{reactant}}} \times 100$$

$$\text{Atom economy (\%)} = \frac{\text{Molecular weight}_{\text{HMF}}}{\text{Molecular weight}_{\text{Glucose}}} \times 100$$

$$\text{Atom economy (\%)} = \frac{126.11}{180.16} \times 100 = \mathbf{70\%}$$

Table S1: Green metrics parameters for conversion of glucose to HMF using FA-CL catalyst.

S. No.	Green metrics parameters	Calculated value
1	Carbon efficiency (%)	64.4
2	<i>E</i> -factor	1.45
3	Atom economy (%)	70

Reaction conditions: Glucose (0.5 g), FA-Cl catalyst (0.05 g), H₂O (5 mL), 145 °C, 6 h.

References

1. C. Emeis, *J. Catal.*, 1993, **141**, 347-354.
2. A. S. Rocha, A. M. Forrester, M. H. de la Cruz, C. T. da Silva and E. R. Lachter, *Catal. Commun.*, 2008, **9**, 1959-1965.
3. V. K. Soni and R. K. Sharma, *ChemCatChem*, 2016, **8**, 1763-1768.